Black carbon solar absorption suppresses turbulence in the atmospheric boundary layer

Thomas, Richard; Bender, Frida; Ramanathan , Veerabhadran; Praveen , Puppala S.; Pistone, Kristina ; Wilcox, Eric

DOI:
10.1073/pnas.1525746113

Document Version
Peer reviewed version

Citation for published version (Harvard):
Thomas, R, Bender, F, Ramanathan , V, Praveen , PS, Pistone, K & Wilcox, E 2016, 'Black carbon solar absorption suppresses turbulence in the atmospheric boundary layer', National Academy of Sciences. Proceedings, vol. 113, no. 42, pp. 11794 – 11799. https://doi.org/10.1073/pnas.1525746113

Black carbon solar absorption suppresses turbulence in the atmospheric boundary layer

Eric M. Wilcox[1], Rick M. Thomas[2,3], P. S. Praveen,[2,4], Kristina Pistone[2,5], Frida A.-M. Bender[6], V. Ramanathan[2]

[1]Division of Atmospheric Sciences, Desert Research Institute, 2215 Raggio Pkwy, Reno, NV 89512, USA; ph: 775-673-7686; email: Eric.Wilcox@dri.edu [2]Center for Clouds, Chemistry and Climate (C[4]), Scripps Institution of Oceanography, Univ. of California, San Diego, 9500 Gilman Dr. MC 0221, La Jolla, CA, 92093-0221, USA [3]School of Geography, Earth and Environmental Sciences, University of Birmingham, Edgbaston, Birmingham, B15 2TT, UK [4]International Centre for Integrated Mountain Development, Khumaltar, Lalitpur, G.P.O. Box 3226, Kathmandu, Nepal. [5] NASA Ames Research Center, Mail Stop 245-5, Moffett Field, CA 94035 [6]Department of Meteorology, Stockholm University, 106 91 Stockholm, Sweden

Submitted to Proceedings of the National Academy of Sciences of the United States of America

The introduction of cloud condensation nuclei and radiative heating by sunlight-absorbing aerosols can modify the thickness and coverage of low clouds yielding significant radiative forcing of climate. The magnitude and sign of changes in cloud coverage and depth in response to changing aerosols are impacted by turbulent dynamics of the cloudy atmosphere, but integrated measurements of aerosol solar absorption and turbulent fluxes have not been made thus far. Here we report the first such integrated measurements made from unmanned aerial vehicles (UAVs) during the CARDEX experiment conducted over the northern Indian Ocean. The UAV and surface data reveal a reduction in turbulent kinetic energy in the surface mixed layer at the base of the atmosphere concurrent with an increase in absorbing black carbon aerosols. Polluted conditions coincide with a warmer and shallower surface mixed layer because of aerosol radiative heating and reduced turbulence. The polluted surface mixed layer was also observed to be more humid with higher relative humidity. Greater humidity enhances cloud development, as evidenced by polluted clouds that penetrate higher above the top of the surface mixed layer. Reduced entrainment of dry air into the surface layer from above the inversion capping the surface mixed layer due to weaker turbulence may contribute to higher relative humidity in the surface layer during polluted conditions. Measurements of turbulence are important for studies of aerosol effects on clouds. Furthermore, reduced turbulence can exacerbate both the human health impacts of high concentrations of fine particles and conditions favorable for low-visibility fog events.

atmospheric turbulence | cloud cover | aerosols | radiative forcing | autonomous unmanned aerial vehicles

\Abstract

The introduction of cloud condensation nuclei and radiative heating by sunlight-absorbing aerosols can modify the thickness and coverage of low clouds yielding significant radiative forcing of climate. The magnitude and sign of changes in cloud coverage and depth in response to changing aerosols are impacted by turbulent dynamics of the cloudy atmosphere, but integrated measurements of aerosol solar absorption and turbulent fluxes have not been made thus far. Here we report the first such integrated measurements made from unmanned aerial vehicles (UAVs) during the CARDEX experiment conducted over the northern Indian Ocean. The UAV and surface data reveal a reduction in turbulent kinetic energy in the surface mixed layer at the base of the atmosphere concurrent with an increase in absorbing black carbon aerosols. Polluted conditions coincide with a warmer and shallower surface mixed layer because of aerosol radiative heating and reduced turbulence. The polluted surface mixed layer was also observed to be more humid with higher relative humidity. Greater humidity enhances cloud development, as evidenced by polluted clouds that penetrate higher above the top of the surface mixed layer. Reduced entrainment of dry air into the surface layer from above the inversion capping the surface mixed layer due to weaker turbulence may contribute to higher relative humidity in the surface layer during polluted conditions. Measurements of turbulence are important for studies of aerosol effects on clouds. Furthermore, reduced turbulence can exacerbate both the human health impacts of high concentrations of fine particles and conditions favorable for low-visibility fog events.

Key words: atmospheric turbulence, cloud cover, aerosols, radiative forcing, autonomous unmanned aerial vehicles

Significance statement

The cooling effect of aerosols on climate and the modification of clouds by aerosols have been widely debated because quantifying their effects is important for constraining current climate change. We present the first-ever measurements of turbulence from unmanned aerial vehicles. We find that absorption of sunlight by black carbon (BC) aerosols suppresses turbulence in the lower atmosphere with important consequences for the environmental impacts of BC emissions from anthropogenic fossil fuel and biomass burning. A mechanism is proposed that links the suppressed turbulence to taller clouds. These results highlight the importance of understanding and observing the role of turbulence in studies of aerosol impacts on clouds. Suppressed turbulence also exacerbates the visibility and human health impacts of pollution.

Black carbon (BC) aerosols associated with the outflow of soot pollution from South Asia spread broadly across the northern Indian Ocean during the winter monsoon season [1]. These

Significance

The cooling effect of aerosols on climate and the modification of clouds by aerosols have been widely debated because quantifying their effects is important for constraining current climate change. We present the first-ever measurements of turbulence from unmanned aerial vehicles. We find that absorption of sunlight by black carbon (BC) aerosols suppresses turbulence in the lower atmosphere with important consequences for the environmental impacts of BC emissions from anthropogenic fossil fuel and biomass burning. A mechanism is proposed that links the suppressed turbulence to taller clouds. These results highlight the importance of understanding and observing the role of turbulence in studies of aerosol impacts on clouds. Suppressed turbulence also exacerbates the visibility and human health impacts of pollution.

Reserved for Publication Footnotes

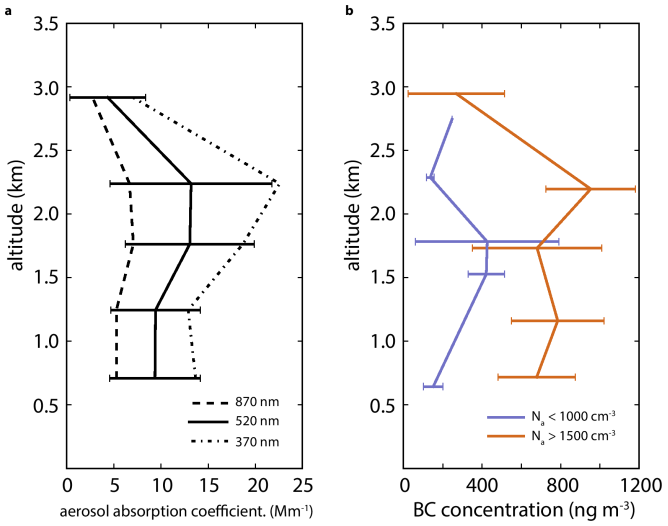

Fig. 1. Profiles of (a) aerosol absorption coefficient at three wavelengths and (b) black carbon (BC) aerosol mass concentration. Blue lines denote profiles when aerosol particle concentration (particles with diameters between 10 nm and 10 μm; denoted N_a) at MCOH is less than 1000 cm^{-3}. Orange lines are for aerosol particle concentration at MCOH greater than 1500 cm^{-3}. Horizontal bars are one standard deviation at each altitude level. Profiles are averages of UAV profiles from 7 days of the more polluted condition and 4 days of the less polluted condition.

BC aerosols directly heat the atmosphere because of absorption of solar radiation [2] and also instantaneously increase the albedo of the clouds [3] from the Twomey effect [4]. Both processes reduce the amount of sunlight reaching the surface, causing a surface cooling of climate. However, changes in low cloud cover, if caused by aerosols, provide perhaps the biggest impact on the net radiative effect of aerosols in this region. While the Twomey effect has been argued to result in an increase in cloud cover [5], the response of turbulence in the boundary layer may play an important role in determining whether aerosol effects result in an increase or decrease in cloudiness [6, 7].

The aerosol absorption in this region is thought to "burn off" the clouds by reducing relative humidity in the cloud layer and suppressing convection, thereby causing a warming of climate by allowing more sunlight to penetrate to the surface [8]. A reduction in low cloudiness, however, is not always the response to lower-tropospheric heating by absorbing soot and smoke aerosols. If the heating reduces turbulent entrainment of dry air from above the humid marine boundary layer, then a thicker layer of cloud can be supported by the greater relative humidity in the surface mixed layer [9, 10]. The result is an enhancement of cloud albedo and a reduction in absorbed solar radiation that partly compensates the increase in net radiative forcing attributable to the dark aerosol residing above a bright cloudy scene [11]. Thus the conceptual view has emerged that BC aerosols within the cloud layer tend to reduce clouds, leading to climate warming, while BC aerosols above the cloud layer tend to increase clouds, leading to climate cooling [12]. These studies, however, have not directly observed the relationship between BC aerosols in the atmosphere and turbulence in the boundary layer. Here we use such measurements to demonstrate how BC aerosols within the cloud layer may reduce turbulence and enhance relative humidity in the cloudy surface mixed layer.

The CARDEX Campaign

We examine the links between black carbon, its solar absorption, and vertical profiles of turbulent fluxes within the boundary layer to understand how the response of turbulence to aerosol forcing impacts clouds. The central component of the Cloud Aerosol Radiative Forcing and Dynamics Experiment (CARDEX) [13] was deployment of lightweight unmanned aerial vehicles (UAVs) for aerosol, radiation, cloud, and turbulent flux measurements [3, 14, 15] advancing the procedures developed in previous UAV studies [2, 3]. The field study was conducted from the Maldives Climate Observatory – Hanimaadhoo [1] (MCOH) during February and March 2012. The existing long-term aerosol and radiation measurements at the observatory were augmented with the UAV aerosol, cloud, and turbulence sampling, as well as a micropulse lidar, a microwave radiometer, and high-frequency wind measurements for near-surface turbulence. The microwave radiometer and near-surface turbulence measurements were made from the top of a 15 m tall tower.

Profiles of the turbulent kinetic energy and vertical flux of latent heat were observed with near-daily UAV flights; the first time such UAV measurements have been applied in studies of aerosol impacts on clouds and climate. The UAV turbulence measurement system has previously been compared with stationary measurements comparable to the tower measurements from MCOH and demonstrated errors of at most 5% [15]. During CARDEX, UAV turbulence data were calculated from sub-sections of 10-15km horizontal flight legs. Sub-section lengths were typically 9.5km and were determined post-flight for each flight as those which captured the full spectral range in covariance ogives and displayed a minimum in wind component variances. At 12-16 times the surface mixed layer height (approx. 600-800m), 9.5km is within the range suggested by [16] required to constrain the accuracy of turbulent variations to within 10%.

The tower measurements of turbulence at MCOH are obtained with a Gill Windmaster pro sonic anemometer and Campbell Krypton-Hygrometer mounted on a mast extending to 23m above the surface. Water vapor fluctuations and 3D wind vectors were logged at 20Hz for the derivation of sensible heat, TKE and water vapor fluxes using eddy covariance methods [17]. TKE was calculated based on all 3 components of the wind velocity. Data processing was performed in 30min averaging periods with despiking to remove points > 3σ of a running 60-second mean and linear detrending was applied. The tower is <75m from the ocean on the northern side of the island, and only data from this wind direction were included in the final analysis.

Profiles of aerosol absorption coefficient and BC aerosol concentration were determined using a miniaturized version of a 3-wavelength absorption photometer [14]. Level flights of 5 to 10 minutes duration are required to reduce random error in the absorption photometer. The BC concentration was determined based on absorption coefficient at 870 nm using an absorption cross section of 10 m^2 g^{-1}. UAV measurements of absorption coefficient in the surface mixed layer agree with simultaneous surface measurements with a commercial aethalometer to within 10% [14].

The aircraft outfitted with aerosol sampling instruments routinely performed profiles up to 3 km altitude from which the profiles of equivalent potential temperature were derived. Level flights at selected heights between 500 m and 3 km were then performed to construct the absorption coefficient and BC aerosol concentration profiles. Profiles from seven flight days were included in the polluted profiles (N_a at MCOH > 1500 cm^{-3}) and profiles from four flight days were included in the cleaner profiles (N_a at MCOH < 1000 cm^{-3}).

The atmospheric boundary layer height was determined using the Mini Micro Pulse Lidar system from SigmaSpace Corp. [18]. In order to distinguish aerosol features confined to the surface mixed layer from elevated aerosol plumes, an upper bound is imposed upon the automated algorithm based on subjective analysis of the backscatter profiles ranging from 900 m to 1700 m depending on the day.

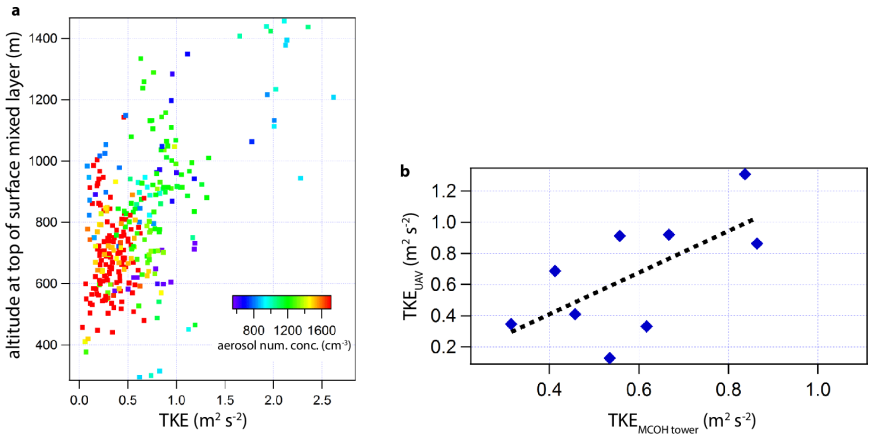

Fig. 2. (a) Altitude at the top of the surface mixed layer estimated from the gradient in micropulse lidar backscatter against turbulent kinetic energy (TKE) measured at the top of the 15 m tower at MCOH. Each sample is colored according to the aerosol particle concentration (particles with diameters between 10 nm and 10 μm) at MCOH. (b) TKE measured by UAV in the upper part of the atmospheric boundary layer against a simultaneous measurement at the MCOH tower.

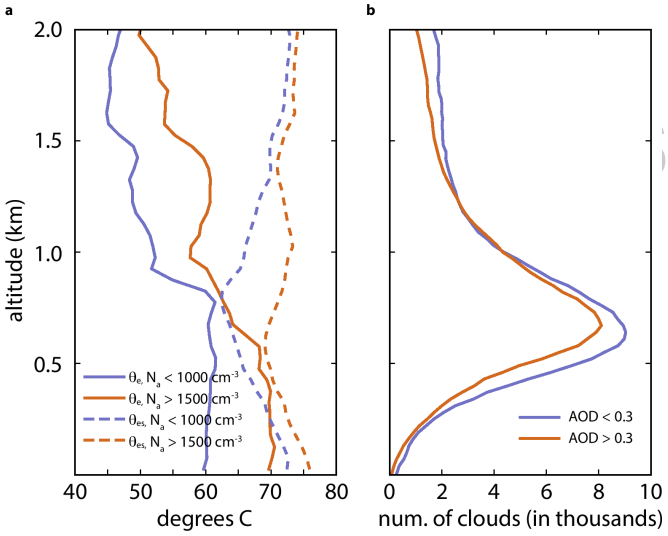

Fig. 3. (a) Profiles of equivalent potential temperature (solid lines) and saturated equivalent potential temperature (dashed lines) measured by UAV. These profiles are averages of the same flights as shown in fig. 1. Blue lines denote profiles when aerosol particle concentration (particles with diameters between 10 nm and 10 μm denoted N_a) at MCOH is less than 1000 cm^{-3}. Orange lines are for aerosol particle concentration at MCOH greater than 1500 cm^{-3}. (b) The number of cloud features observed by the CALIOP lidar on the Calipso satellite. Data are from all passes of Calipso during February 2007 to 2013 and all samples within 5 degrees lat/lon around MCOH. Blue line denotes profiles where the aerosol optical depth (AOD) is less than 0.3 (the median value) observed by the Moderate Resolution Imaging Spectroradiometer (MODIS) instrument on the Aqua satellite flying in formation with Calipso. The orange line denotes profiles where the AOD is greater than 0.3.

Results

During the winter monsoon there is a well-mixed atmospheric layer above the northern Indian Ocean, referred to here as the surface mixed layer, which extends from the ocean surface to a strong capping inversion the surface layer below 1 km altitude. At the top of the surface mixed layer the potential temperature increases by 2 K or more in 100 m vertical distance and the relative humidity decreases from about 75% within the surface mixed layer to about 50% on average (and often much lower) in the drier layer above. The bases of small cumulus clouds reside at the top of the surface mixed layer and penetrate into the inversion, as is typical for trade wind cumulus cloud regions. However, in many such locations the cloud tops range from just above the top of the surface mixed layer to as high as 3 km where a weaker temperature inversion, known as the trade wind inversion, occurs [19]. In contrast, the dry stable layer above the capping inversion prevents the weak cumulus clouds over the northern Indian Ocean from penetrating much further above the inversion at the top of the surface mixed layer and cloud fraction is typically less than 0.1.

The mean profile of the aerosol absorption coefficient peaks at approximately 2 km altitude (Fig. 1a). The soot layer containing the BC aerosol extends on average from the surface up to 3 km altitude, although there is considerable daily variability in the structure of the profile. Pollution occurs more frequently above 1500 m altitude when the origin of the lower-tropospheric flow is over the continent, and often the particle concentration at the surface also increases during these periods [14]. Through the dry winter monsoon season the increase in surface pollution is indicative of transport in the column up to 3 km [1]. This increase in aerosol optical depth (AOD) coincides with an increase in the absorption coefficient and a decrease in aerosol single scattering albedo [1] that are attributed to continental pollution characterized by high concentrations of submicron absorbing aerosol [20].

The BC aerosol concentration profiles from eleven flight days were sorted according to particle concentration measurements at the surface. They show that the BC concentration was substantially greater up to 3 km altitude with increased pollution at the surface (Fig 1b). The mean absorption coefficient at 2 km shown in Fig. 1 is comparable in magnitude to the profile reported during the polluted episode of the previous Maldives Airborne Campaign (MAC; [2, 14]), but is substantially larger in the atmospheric boundary layer below 1.5 km, compared to MAC. The diurnally-averaged solar heating rate of the atmosphere at 2 km altitude was estimated at nearly 1 K d^{-1} based on direct observations of convergence of solar flux between stacked UAVs during the MAC polluted period [2]. The average aerosol heating rate during CARDEX was therefore likely comparable during polluted episodes. Aerosol heating within the surface mixed layer may be greater than the approximately 0.2 K d^{-1} estimated during the MAC polluted episode because of the greater absorption coefficient in the surface mixed layer during CARDEX. During the Indian Ocean Experiment (INDOEX), solar absorption in the aerosol layer was estimated to cause a reduction in surface solar flux of -18 W m^{-2}, and aerosol scattering an additional -2 W m^{-2} at the surface [21]. Thus the northern Indian Ocean is characterized by a deep layer of BC aerosols contributing a heating from within the surface mixed layer to an altitude of up to 3 km. Shallow cumulus clouds are embedded within the BC aerosol layer [3, 22].

The turbulent kinetic energy (TKE) and height of the top of the surface mixed layer are shown in Fig. 2a as a scatter plot where the color of the points indicates the particle concentration

Table 1. Linear regression analysis of daytime relative humidity (RH) at 1000 hPa with dynamical parameters in Feb. and Mar. 2006-2012 ECMWF ERA-Interim reanalysis at the model grid cell corresponding to the MCOH station. Correlation coefficients (r) shown with sign of the relationship. Correlations of dynamical parameters with surface particle concentration (N_a) and differences between more polluted and less polluted conditions are based on particle concentration measurements from the 2006 and 2012 seasons.

Reanalysis parameter	correlation with RH at 1000 hPa	correlation with surface particle concentration	difference between N_a > 1500 cm^{-3} and N_a <1000 cm^{-3}
vertical vel. at 925 hPa	-0.30	-0.05	-0.012 Pa s^{-1}
vertical vel. at 750 hPa	-0.25	0.05	-0.013 Pa s^{-1}
u vel. at 750 hPa	-0.21	-0.07	-0.87 m s^{-1}
divergence at 1000 hPa	-0.21	-0.18	-3.0 x 10^{-6} s^{-1}
divergence at 750 hPa	-0.07	-0.12	-3.7 x 10^{-7} s^{-1}
u vel. at 1000 hPa	-0.05		
v vel. at 750 hPa	0.02		
v vel. at 1000 hPa	0.01		
pot. temp. difference 750 hPa minus 1000 hPa	0.03		
geopotential at 500 hPa	0.07		

near the surface. As pollution increased at MCOH (indicated by yellow and red colored samples), TKE decreased. A reduction in TKE inhibits the upward mixing of the surface mixed layer top by entrainment of dry air from above the inversion into the surface layer. Therefore, the altitude of the surface mixed layer top was lower during the polluted periods of decreased TKE. In addition to the surface measurements, TKE was profiled through the surface mixed layer by UAV. We find that TKE above the surface and in the surface mixed layer roughly correlates with surface measurements of TKE (Fig. 2b) suggesting that the reduced turbulence during polluted conditions extends through this layer.

The inversion capping the surface mixed layer is characterized by a decrease in equivalent potential temperature (θ_e) above the surface layer with nearly uniform θ_e (solid lines, Fig. 3a). The polluted conditions during CARDEX coincided with a lower capping inversion at approximately 600 m altitude (orange solid line, Fig. 3a) compared to approximately 800 m altitude during cleaner conditions (blue solid line, Fig. 3a), consistent with the lower boundary layer top altitude indicated by the micropulse lidar in Fig. 2a above.

Polluted conditions also corresponded to a warmer and more humid surface mixed layer, which is indicated by a greater θ_e compared to cleaner conditions. Boundary layer temperature was greater by about 1 K during polluted conditions compared to cleaner conditions and the mean surface relative humidity increased from 69.7% during cleaner conditions to 77.4% during polluted conditions. In spite of the lower altitude of the surface mixed layer top during polluted conditions, the layer of nearly saturated air conducive to cloud formation (where $\theta_e = \theta_{es}$) was thicker during more polluted conditions compared to less polluted conditions. Multi-year observations of cloud-top height from the NASA Cloud-Aerosol Lidar with Orthogonal Polarization (CALIOP) satellite lidar confirm that cloud tops are almost uniformly confined to within a few hundred meters of the surface mixed layer top (Fig. 3b). The CALIOP vertical feature mask (version 3) [23] [24] profiles have been sorted according to multi-year observations of AOD from the Moderate Resolution Imaging Spectroradiometer (MODIS) to separate the number of observed cloud tops when AOD is less than the median value over MCOH (0.3) from the number of cloud tops when AOD is greater than the median value. Approximately 100 overpasses of the CALIOP instrument are included here comprising every overpass within approximately 250 km of MCOH during February and March for years 2007 through 2013. Regardless of the amount of aerosol, most of the cloud tops reside between 400 m and 1200 m altitude with the peak occurrence of cloud tops between 600 m and 700 m. In spite of the reduction in turbulence and lowering of the top of the surface mixed layer by at least 200 m, the altitude of the cloud tops is similar between the less polluted and more polluted conditions. During the cleaner conditions clouds do not have sufficient buoyancy to penetrate the inversion and CALIOP shows that most of the cumulus cloud tops are observed to reside below the elevation of the inversion observed during CARDEX. In contrast, during polluted conditions, most of the cloud tops reside above the elevation of the inversion indicating greater vertical cloud development allowed by the more humid polluted conditions. Although the CALIOP data are from a multi-year climatology, the result is consistent with a companion study showing increasing cloud liquid water path with increasing aerosol for clouds observed with a ground-based microwave radiometer during the CARDEX period [25]. Both the CALIOP result and the microwave radiometer result are consistent with the thicker saturated layer under more polluted conditions shown in Fug 3b.

Discussion

The conceptual picture that emerges from these observations is one whereby aerosol absorption heats the boundary layer and lower troposphere under polluted conditions. A reduction in boundary layer turbulent kinetic energy decreases the entrainment of air across the temperature inversion at the top of the boundary layer, which favors a lower surface mixed layer top. The reduced turbulence might initially suppress cloud development, however the reduced turbulent mixing across the inversion also leads to greater relative humidity in the surface mixed layer because of weakened mixing of moist air up through the interface and weakened mixing of dry tropospheric air down into the mixed layer. Thus the vertical profile shifts from a condition where clouds are confined to the top of the surface mixed layer to a condition where clouds form in a thicker saturated layer and may

penetrate above the inversion because greater humidity provides additional buoyancy.

Large-eddy simulations of the response of northern Indian Ocean cumulus clouds to heating by absorbing aerosols previously indicated that heating within the cloud layer can reduce relative humidity and low cloud cover, thus contributing a positive semi-direct radiative heating during the winter monsoon [8]. Long-term records of low clouds suggest that a slight increase in cloud cover occurred over the northern Indian Ocean during a time when aerosol emissions were increasing [26]. Remote sensing data suggests that low cloud cover increases with increasing aerosol optical thickness for small amounts aerosol and decreases with increasing aerosol optical thickness for large amounts of aerosol [27] [28]. Thus the response of low clouds to BC aerosol absorption may depend on the amount of aerosol present. Enhancement of cloud development and lowering of the boundary layer top due to aerosol heating above clouds has been observed over the Southeast Atlantic Ocean [10]. While the consequences of BC absorption for the coverage of clouds was not measured during CARDEX, the enhanced humidity and thicker saturated cloud layer observed during the more polluted conditions of CARDEX suggest that same process may impact trade cumulus clouds within a layer of absorbing aerosol, as was observed for Southeast Atlantic clouds beneath absorbing aerosols, at least for the conditions observed during CARDEX.

The consequences of BC aerosols for radiative forcing of climate depends on balances among the direct aerosol radiative heating, increases in cloud drop concentrations [22, 3], as well as the changes in turbulence and relative humidity described here. Further study is required to account for the full range in variability in BC aerosol loading and the combined radiative effects of changes in cloud microphysics, changes in cloud development in response to reduced turbulence, and changes in cloud cover with increasing aerosol.

The observations available from CARDEX are suggestive of a mechanism by which absorbing aerosols can lead to increased humidity rather than decreased humidity in the surface mixed layer where cumulus cloud updrafts originate. We note that such relationships among observed aerosol amounts, TKE, humidity and temperature are not on their own sufficient to rule out the possibility that the atmospheric dynamics leading to increasing aerosol also leads to a warmer and more humid surface mixed layer independently of the aerosols. Further modeling experiments are certainly warranted to isolate the impact of aerosols from these additional factors. We note, that heating of the aerosol layer by BC aerosol absorption has been measured directly and independently of meteorological influence [2] and also that the more polluted air masses have their origins over the continent, while the less polluted air masses originate over the ocean [29]. Based on air mass history, one might expect that more polluted air masses would be warmer and drier than the less polluted air masses. Our proposed mechanism explains why the expected result is not what is observed and also why the expected reduction in cloud cover due to BC aerosols is not apparent in prior studies of remote sensing and long-term surface data.

To further explore the possibility that regional dynamics may lead to a coincidental moistening of the surface mixed layer with increasing aerosol independent of the aerosol radiative impact on turbulence described above, a linear regression analysis has been performed with the ECMWF ERA-Interim reanalysis dataset [30]. Table 1 shows the linear correlation between the daytime relative humidity at 1000 hPa and the winds, divergence, static stability, and geopotential height from 7 years of Feb. and Mar. ECMWF data for the model grid cell located over the MCOH field station. The analysis shows shows that: 1) 1000 hPa relative humidity is not strongly correlated with any of the metrics examined; 2) that the strongest correlations are with the vertical velocity and divergence fields at 1000 hPa and 750 hPa; and 3) the differences in vertical velocity and divergence between more polluted conditions and less polluted conditions are small relative to the dynamic range of these quantities. These differences in zonal (u) velocity, vertical velocity and divergence, even if independent, would together explain only about 1% to 2% of the approximately 8% increase in relative humidity between more polluted and less polluted conditions. Furthermore, the vertical velocity and divergence parameters are neither independent of one another nor independent of the local turbulent dynamics in the boundary layer. These results do not suggest a strong dynamical effect related to the large-scale dynamics, at least in the ECMWF reanalysis, that might explain a coincidental increase relative humidity in the surface mixed layer with transport of BC aerosols to the experiment location. However, further modeling is required to isolate the impact of aerosols from other meteorological impacts on surface mixed layer properties.

The shallow cumulus clouds observed over the northern Indian Ocean are embedded within a deep layer of BC aerosols. The response of boundary layer turbulence and clouds may depend on the vertical orientation of the absorbing aerosols relative to the cloud layer, as well as the response of the clouds themselves. For example, in the Amazon where deeper cumulus clouds are embedded in absorbing BC aerosols [31] find that the introduction of BC aerosols in a model experiment reduces TKE below the aerosol layer and increases TKE in a narrow layer above the aerosol layer. At low aerosol amounts, increasing aerosol leads to taller clouds, while at high aerosol amounts, increasing aerosol leads to reduced cloudiness. In one model experiment a reduction in latent heat flux from the surface due to high aerosol was sufficient to substantially reduce cloud cover [32]. These results are broadly consistent with satellite observations over the Amazon [33]. The model-simulated reduction in TKE for the Amazon case is similar to our observations over the Indian Ocean. However, the increase in cloud depth over the Amazon for low aerosol amounts is argued to be a consequence of microphysical impacts of aerosol on clouds, which is not likely to be a factor over the northern Indian Ocean. The mechanisms cited for invigoration of clouds by aerosols include suppression of rainfall and a related addition of latent heat from freezing of liquid drops. Even the cleanest clouds we have observed are composed of drops that are too small to contribute to drizzle [3]. Furthermore, the clouds are too shallow to contain ice. Simulated stratocumulus clouds with absorbing aerosol entirely above the cloud layer exhibited a thickening of the cloud due to reduced entrainment of dry air into the cloud layer at cloud top [9]. TKE may in fact be enhanced in the boundary layer for absorbing aerosol above stratocumulus due to the greater condensed water in the overcast cloud layer. Nevertheless, entrainment is reduced due to the increase in buoyancy of the aerosol layer above the cloud. Thus the mechanism for thickening cloud over the southeast Atlantic Ocean may be slightly different than we are proposing here for the northern Indian Ocean.

Suppression of boundary layer turbulence by BC aerosols can lead to additional impacts beyond changes in cloud radiative forcing. High relative humidity and large particle concentrations are related to low-visibility fog events [34], which have increased in frequency and duration over South Asia [35] [36]. Furthermore, reduced vertical mixing and a lowering of the boundary layer top will increase the surface number concentration of BC particles, which are known to have substantial negative impacts on human health in South Asia [37] [38].

[1 V. Ramanathan, F. Li, M. V. Ramana, P. S. Praveen, D. Kim, C. E. Corrigan and H. Nguyen,

"Atmospheric Brown Clouds: Hemispherical and regional variations in long range transport, absorption, and radiative forcing," *J. Geophys. Res.,* vol. 112, p. D22S21, 2007.
[2 V. Ramanathan, M. V. Ramana, G. Roberts, D. Kim, C. E. Corrigan, C. E. Chung and W. D., "Warming trends in Asia amplified by brown cloud solar absorption," *Nature,* vol. 448, pp. 575-578, 2007.
[3 G. C. Roberts, M. V. Ramana, C. Corrigan, D. Kim and V. Ramanathan, "Simultaneous observations of aerosol-cloud-albedo interactions with three stacked unmanned aerial vehicles," *PNAS,* vol. 105, no. 21, pp. 7370-7375, 2008.
[4 S. Twomey, "The influence of pollution on the shortwave albedo of clouds," *J. Atmos. Sci.,* vol. 34, pp. 1149-1152, 1977.
[5 B. A. Albrecht, "Aerosols, cloud microphysics, and fractional cloudiness," *Science,* vol. 245, pp. 1227-1230, 1989.
[6 A. S. Ackerman, K. M. P., D. E. Stevens and O. B. Toon, "The impact of humidity above stratiform clouds on indirect aerosol climate forcing," *Nature,* vol. 432, pp. 1014-1017, 2004.
[7 B. Stevens and G. Feingold, "Untangling aerosol effects on clouds and precipitation in a buffered system," *Nature,* vol. 461, pp. 607-613, 2009.
[8 A. S. Ackerman, O. B. Toon, D. E. Stevens, A. J. Heymsfield, V. Ramanathan and E. J. Welton, "Reduction of tropical cloudiness by soot," *Science,* vol. 288, pp. 1042-1047, 2000.
[9 B. T. Johnson, K. P. Shine and P. M. and Forster, "The semi-direct aerosol effect: Impact of absorbing aerosols on marine stratocumulus," *Q. J. Roy. Meteorol. Soc.,* vol. 130, p. 1407–1422, 2004.
[10 E. M. Wilcox, "Stratocumulus cloud thickening beneath layers of absorbing smoke aerosol," *Atmos. Chem. Phys.,* vol. 10, p. 11769– 11777, 2010.
[11 E. M. Wilcox, "Direct and semi-direct radiative forcing of smoke aerosols over clouds," *Atmos. Chem. Phys.,* vol. 12, p. 139–149, 2012.
[12 D. Koch and A. D. D. Genio, "Black carbon semi-direct effects on cloud cover: review and synthesis," *Atmos. Chem. Phys.,* vol. 10, p. 7685–7696, 2010.
[13 V. Ramanathan, R. M. Thomas, P. S. Praveen, H. Nguyen, E. Wilcox, F. Bender and K. Pistone, 2011. [Online]. Available: http://ramanathan.ucsd.edu/files/CARDEX_prop_Jun_20.pdf.
[14 C. E. Corrigan, G. C. Roberts, M. V. Ramana, D. Kim and V. Ramanathan, "Capturing vertical profiles of aerosols and black carbon over the Indian Ocean using autonomous unmanned aerial vehicles," *Atmos. Chem. Phys.,* vol. 8, p. 737–747, 2008.
[15 R. Thomas, K. Lehman, H. Nguyen, D. Jackson, D. Wolfe and V. Ramanathan, "Measurement of turbulent water vapor fluxes using a lightweight unmanned aerial vehicle system," *Atmos. Meas. Tech.,* vol. 4, pp. 5529-5568, 2011.
[16 D. H. Lenschow and B. Stankov, "Length scales in the convective boundary layer," *J. of the Atmos. Sci.,* vol. 43, no. 12, pp. 1198-1209, 1986.
[17 T. Foken, Micrometeorology, C. J. Nappo, Ed., Springer, 2008, p. 306.
[18 I. M. Brooks, "Finding Boundary Layer Top: Application of a Wavelet Covariance Transform to Lidar Backscatter Profiles," *J. Atmos. Oceanic Technol.,* vol. 20, pp. 1092-1105, 2003.
[19 B. Medeiros, L. Nuijens, C. Antoniazzi and B. Stevens, "Low-latitude boundary layer clouds as seen by CALIPSO," *J. Geophys. Res.,* vol. 115, p. D23207, 2010.
[20 C. E. Corrigan, V. Ramanathan and a. J. J. Schauer, "Impact of monsoon transitions on the physical and optical properties of aerosols," *Journal of Geophysical Research: Atmospheres,* vol. 111, p. D18208, 2006.
[21 V. Ramanathan, P. J. Crutzen, J. Lelieveld, A. P. Mitra, D. Althausen and e. al., "Indian Ocean Experiment: An integrated analysis of the climate forcing and effects of the great Indo-Asian haze," *J. Geophys. Res.,* vol. 106, pp. 28,371–28,398, 2001.
[22 A. J. Heymsfield and G. M. McFarquhar, "Microphysics of INDOEX clean and polluted trade cumulus clouds," *J. Geophys. Res.,* vol. 106, no. D22, pp. 28,653-28,673, 2001.
[23 Z. Liu, M. Vaughan, D. Winker, C. Kittaka, B. Getzewich, R. Kuehn, A. Omar, K. Powell, C. Trepte and C. Hostetler, "The CALIPSO lidar cloud and aerosol discrimination: Version 2 algorithm and initial assessment of performance," *J. Atmos. Oceanic Technol.,* vol. 26, p. 1198– 1213, 2009.
[24 D. M. Winker, M. A. Vaughan, A. Omar, Y. Hu, Powell, K. A., Z. Liu, W. H. Hunt and S. A. Young, "Overview of the CALIPSO Mission and CALIOP Data Processing Algorithms," *J. Atmos. 25 Oceanic Technol.,* vol. 26, p. 2310–2323, 2009.
[25 K. Pistone, P. S. Praveen, R. M. Thomas, V. Ramanathan, E. M. Wilcox and F. A.-M. Bender, "Observed correlations between aerosol and cloud properties in an Indian Ocean trade cumulus regime," *Atmos. Chem. Phys.,* vol. 16, pp. 5203-5227, 2016.
[26 J. Norris, "Has northern Indian Ocean cloud cover changed due to increasing anthropogenic aerosol?," *Geophys. Res. Lett.,* vol. 28, pp. 3271-3274, 2001.
[27 S. Dey, L. Di Girolamo, ,. G. Zhao, A. L. Jones and G. M. McFarquhar, "Satellite-observed relationships between aerosol and trade-wind cumulus cloud properties over the Indian Ocean," *Geophys. Res. Lett.,* vol. 38, p. L01804, 2011.
[28 Y. Kaufman and I. Koren, "Smoke and Pollution Aerosol Effect on Cloud Cover," *Science,* vol. 313, no. 5787, pp. 655-658, 2006.
[29 F. F. Höpner, F. A.-M. Bender, A. M. L. Ekman, P. S. Praveen, C. Bosch, J. A. Ogren, A. Andersson, Ö. Gustafsson and a. V. Ramanathan, "Vertical profiles of optical and microphysical particle properties above the northern Indian Ocean during CARDEX 2012," *Atmos. Chem. Phys.,* vol. 16, pp. 1045-1064, 2016.
[30 D. Dee, S. Uppala, A. Simmons, P. Berrisford, P. Poli, S. Kobayashi, U. Andrae, M. Balmaseda, G. Balsamo, P. Bauer and P. Bechtold, "The ERA-Interim reanalysis: Configuration and performance of the data assimilation system," *Quarterly Journal of the Royal Meteorological Society,* vol. 137, no. 656, pp. 553-597, 2011.
[31 J. E. Ten Hoeve, M. Z. Jacobson and a. L. A. Remer, "Comparing results from a physical model with satellite and in situ observations to determine whether biomass burning aerosols over the Amazon brighten or burn off clouds," *J. Geophys. Res.,* vol. 117, p. D08203, 2012.
[32 G. Feingold, H. Jiang and J. Harrington, "On smoke suppression of clouds in Amazonia," *Geophysical Research Letters,* vol. 32, no. 2, p. L02804, 2005.
[33 I. Koren, J. V. Martins, L. A. Remer and &. H. Afargan, "Smoke invigoration versus inhibition of clouds over the Amazon," *Science,* vol. 321, pp. 946-949, 2008.
[34 R. Gautam, N. C. Hsu, M. Kafatos and S.-C. Tsay, "Influences of winter haze on fog/low cloud over the Indo-Gangetic plains," *J. Geophys. Res.,* vol. 112, p. D05207, 2007.
[35 R. K. Jenamani, "Alarming rise in fog and pollution causing a fall in maximum temperature over Delhi," *Current Science,* vol. 93, no. 3, pp. 314-322, 2007.
[36 F. S. Syed, K. H and M. Tjernström, "On the fog variability over south Asia," *Clim. Dyn.,* vol. 39, pp. 2993-3005, 2012.
[37 N. A. Janssen, G. Hoek, M. Simic-Lawson, P. Fischer, L. v. Bree, M. K. H. ten Brink, H. R. A. R. W. Atkinson, B. Brunekreef and F. R. Cassee, "Black Carbon as an Additional Indicator of the Adverse Health Effects of Airborne Particles Compared with PM10 and PM2.5," *Environ. Health Perspect.,* vol. 119, pp. 1691-1699, 2011).
[38 K. R. Smith, "National burden of disease in India from indoor air pollution.," *Proc. Natl Acad. Sci.,* vol. 97, p. 13286–13293, 2005.

Acknowledgments

We acknowledge the NSF for supporting the CARDEX campaign through grant NSF-0721142. We also thank Hung Nguyen for expert project and flight management for CARDEX. E.M.W. acknowledges the Desert Research Institute for support to participate in CARDEX and NASA grant NNX11AG89G. **Author Contributions** E.M.W. wrote the paper. V.R., R.M.T., P.S.P., E.M.W., K.P., and F.A.-M.B. designed and executed CARDEX. V.R. was the principal investigator with E.M.W. the co-principal investigator. R.M.T was the lead instrument scientist for the surface and UAV turbulence measurements. P.S.P was the lead instrument scientist for the surface and UAV aerosol measurements. F.A.-M.B. was the lead instrument scientist for the micropulse lidar measurements. All authors reviewed and commented on the paper.

We acknowledge the NSF for supporting the CARDEX campaign through grant NSF-0721142. We also thank Hung Nguyen for expert project and flight management for CARDEX. E.M.W. acknowledges the Desert Research Institute for support to participate in CARDEX and NASA grant NNX11AG89G.
Author Contributions
E.M.W. wrote the paper. V.R., R.M.T., P.S.P., E.M.W., K.P., and F.A.-M.B. designed and executed CARDEX. V.R. was the principal investigator with E.M.W. the co-principal investigator. R.M.T was the lead instrument scientist for the surface and UAV turbulence measurements. P.S.P was the lead instrument scientist for the surface and UAV aerosol measurements. F.A.-M.B. was the lead instrument scientist for the micropulse lidar measurements. All authors reviewed and commented on the paper.